Received: 7 June 2023 | Revised: 20 August 2023 | Accepted: 23 August 2023

DOI: 10.1002/ajh.27088

RESEARCH ARTICLE

A novel missense variant in *ATP11C* is associated with reduced red blood cell phosphatidylserine flippase activity and mild hereditary hemolytic anemia

Myrthe J. van Dijk[1,2] | Brigitte A. van Oirschot[1] | Alexander N. Harrison[3] | Steffen M. Recktenwald[4] | Min Qiao[4,5] | Amaury Stommen[6] | Anne-Sophie Cloos[6] | Juliette Vanderroost[6] | Romano Terrasi[7] | Kuntal Dey[8] | Jennifer Bos[1] | Minke A. E. Rab[1,9] | Anna Bogdanova[8] | Giampaolo Minetti[10] | Giulio G. Muccioli[7] | Donatienne Tyteca[6] | Stéphane Egée[11] | Lars Kaestner[4,5] | Robert S. Molday[3] | Eduard J. van Beers[2] | Richard van Wijk[1]

[1]Central Diagnostic Laboratory—Research, University Medical Center Utrecht, Utrecht University, Utrecht, The Netherlands

[2]Center for Benign Hematology, Thrombosis and Hemostasis—Van Creveldkliniek, University Medical Center Utrecht, Utrecht University, Utrecht, The Netherlands

[3]Department of Biochemistry and Molecular Biology, University of British Columbia, Vancouver, Canada

[4]Department of Experimental Physics, Saarland University, Saarbrücken, Germany

[5]Theoretical Medicine and Biosciences, Saarland University, Homburg, Germany

[6]CELL Unit and PICT Platform, de Duve Institute, UCLouvain, Brussels, Belgium

[7]Bioanalysis and Pharmacology of Bioactive Lipids Research Group, Louvain Drug Research Institute, UCLouvain, Brussels, Belgium

[8]Red Blood Cell Group, Institute of Veterinary Physiology, University of Zurich, Zurich, Switzerland

[9]Department of Hematology, Erasmus Medical Center Rotterdam, Rotterdam, The Netherlands

[10]Department of Biology and Biotechnology "L. Spallanzani", Laboratories of Biochemistry, University of Pavia, Pavia, Italy

[11]UMR 8227 CNRS-Sorbonne Université, Station Biologique de Roscoff, Roscoff, France

Abstract

Adenosine Triphosphatase (ATPase) Phospholipid Transporting 11C gene *(ATP11C)* encodes the major phosphatidylserine (PS) flippase in human red blood cells (RBCs). Flippases actively transport phospholipids (e.g., PS) from the outer to the inner leaflet to establish and maintain phospholipid asymmetry of the lipid bilayer of cell membranes. This asymmetry is crucial for survival since externalized PS triggers phagocytosis by splenic macrophages. Here we report on pathophysiological consequences of decreased flippase activity, prompted by a patient with hemolytic anemia and hemizygosity for a novel c.2365C > T p.(Leu789Phe) missense variant in *ATP11C*. ATP11C protein expression was strongly reduced by 58% in patient-derived RBC ghosts. Furthermore, functional characterization showed only 26% PS flippase activity. These results were confirmed by recombinant mutant ATP11C protein expression in HEK293T cells, which was decreased to 27% compared to wild type, whereas PS-stimulated ATPase activity was decreased by 57%. Patient RBCs showed a mild increase in PS surface exposure when compared to control RBCs, which further increased in the most dense RBCs after RBC storage stress. The increase in PS was not due to higher global membrane content of PS or other phospholipids. In contrast, membrane lipid lateral distribution showed increased abundance of cholesterol-enriched domains in RBC low curvature areas. Finally, more dense RBCs and subtle changes in RBC morphology under flow hint toward alterations in flow behavior of ATP11C-deficient RBCs. Altogether, ATP11C deficiency is the likely cause of hemolytic anemia in our patient, thereby underlining the physiological role and relevance of this flippase in human RBCs.

Correspondence
Richard van Wijk, Heidelberglaan 100, 3584 CX, Utrecht, The Netherlands.
Email: r.vanwijk@umcutrecht.nl

1 | INTRODUCTION

Hereditary hemolytic anemia encompasses a group of inherited conditions characterized by premature destruction of red blood cells (RBCs). They can be broadly classified as hemoglobin (Hb) disorders, RBC enzyme disorders, or RBC membrane disorders. In the latter, modifications in membrane proteins may disrupt membrane mechanical integrity, stability, and RBC deformability.[1]

Membrane proteins are essential to establish and maintain phospholipid asymmetry of the lipid bilayer of cell membranes. Indeed, phosphatidylserine (PS) and phosphatidylethanolamine (PE) are restricted primarily to the inner leaflet, whereas phosphatidylcholine (PC) and sphingomyelin are exposed on the cell surface.[2] Maintenance of this asymmetric distribution is ensured by flippases, floppases, and scramblases. Flippases actively transport phospholipids (e.g., PS) from the outer to the inner leaflet.[3–6] The major flippase in human RBCs, Adenosine Triphosphatase (ATPase) Phospholipid Transporting 11C (ATP11C), forms a complex with transmembrane protein cell cycle control protein 50A (CDC50A, also known as TMEM30A).[7–10] PS internalization reduces the "eat me" signal for phagocytosis by macrophages of the reticuloendothelial system, especially in the spleen.[5] Conversely, ATP-binding cassette (ABC) transporter floppases actively transport phospholipids at a slower rate in the opposite direction, whereas calcium (Ca^{2+})-dependent scramblases facilitate passive transportation in both directions.[3]

Senescent RBCs show decreased flippase activity, while scramblase activity remains unchanged. This contributes to increased PS surface exposure, signaling splenic macrophages.[11] In a wide variety of RBC disorders, including sickle cell disease and thalassemia, increased PS surface exposure is associated with hemolytic anemia.[12,13] In addition, exposing PS on the RBC surface can lead to increased RBC adhesion to vascular endothelial cells and activation of surface-dependent plasma blood-clotting factors.[14] Moreover, as the interplay of PS with the spectrin-based membrane skeleton is crucial for mechanical stability of RBCs,[3,15,16] one could expect alteration of this RBC parameter as well. This is reflected by studies in ATP11C deficient mice and the one human patient identified to date with an *ATP11C* variant.[17,18]

Here we study the effects of ATP11C deficiency and report on a patient with hemizygosity for a novel c.2365C > T p.(Leu789Phe) variant in *ATP11C*. Functional analysis of patient RBCs and recombinant mutant murine protein provide convincing evidence for the pathogenic nature of the identified missense variant and the pathophysiological consequences of decreased RBC flippase activity, and thereby hemolytic anemia observed in the patient. In addition, our findings lead to a better understanding of the physiological role and important function of ATP11C in human RBCs.

2 | METHODS

2.1 | Patient and control samples

After obtaining informed consent (Netherlands Trial Register NTR6462, approved by the Medical Research Ethics Committee Utrecht, The Netherlands, no. 17/450, in accordance with the Declaration of Helsinki), peripheral blood samples from the patient were collected into tubes with ethylenediaminetetraacetic acid or heparin as anticoagulant at three outpatient visits in 2019, 2021, and 2022. The mother's blood was also analyzed for presence of the variant. Control blood samples ($n = 7$ in total), if needed age- and gender-matched, were collected through the Mini Donor Service of the University Medical Center Utrecht, The Netherlands. After collection, part of the tubes were transferred by cooled transport to other research laboratories in Europe.

2.2 | Mutation analysis of *ATP11C*

Genomic DNA was extracted from peripheral blood of the patient using standard procedures.[19] Targeted next generation gene panel sequencing was performed as part of the diagnostic work-up for hereditary hemolytic anemia on 46 genes including *ATP11C* (Table S1). Genetic analysis of the mother's DNA was performed by sequencing of *ATP11C* only.

2.3 | Recombinant mutant ATP11C

Recombinant mutant ATP11C protein was generated by site directed mutagenesis of the equivalent residue (Leu786) in murine *Atp11c* cDNA. Mutant and wild type (WT) proteins were transiently expressed in HEK293T cells. Expression levels were determined by immunoblotting after solubilization with 3-cholamidopropyl dimethylammonio 1-propanesulfonate (CHAPS; Anatrace) detergent. PS titration ATPase activity assays were performed on detergent-solubilized protein with the same number of cells used in each experiment. Single point ATPase activity of the purified protein in presence of 100% 1,2-dioleoyl-sn-glycero-3-phosphocholine (DOPC; Avanti Polar Lipids) versus 20% 1,2-dioleoyl-sn-glycero-3-phosphoserine (DOPS; Avanti Polar Lipids) and 80% DOPC was measured to analyze functional properties of Leu786 mutants.[20] ATPase activity was studied by comparing the rate of ATP hydrolysis in 20% DOPS and 80% DOPC with the rate in 100% DOPC. Maximum activity (V_{max}) and Michaelis–Menten constant (K_m) were calculated using Michaelis-Menton kinetics in Prism 7 (GraphPad Software).

2.4 | Immunoblotting of human RBCs

ATP11C protein expression was determined in RBC ghosts by immunoblotting. RBCs were purified using columns with cellulose (1:1 w/w α-cellulose and cellulose type 50 [Sigma-Aldrich] in NaCl 0.9%).[21] RBC ghosts were prepared by lysing RBCs with hypotonic phosphate buffer (1.4 mM NaH_2PO_4, 5.7 mM Na_2HPO_4) supplemented with complete protease inhibitor cocktail (Roche). This was followed by washing steps (21 000 g, no brake) till pellets were free of Hb. Protein concentration was measured by the Bradford method using Protein Assay Dye Reagent Concentrate (Bio-rad). Equal protein amounts were electrophoresed by sodium dodecylsulfate polyacrylamide gel electrophoresis (SDS-PAGE) on a 4%–12% gradient gel and transferred to a polyvinylidene difluoride (PVDF) membrane. This PVDF membrane was blocked with Odyssey Blocking Buffer (LI-COR) in phosphate buffered saline (PBS; Sigma-Aldrich) and incubated with: anti-ATP11C (Rat IgG; 1:50; conditioned medium 11C4 clone [gift Prof. Namakura, Tokyo Women's Medical University]) and anti-actin (Mouse IgM; 1:5000 [Calbiochem CP01]). Blots were visualized using Alexa Fluor® 680-conjugated Goat anti-Rat IgG and Goat anti-Mouse IgM antibodies (LI-COR) and quantified using the Odyssey Infrared Imaging System. Levels of ATP11C were evaluated relative to the intensity of actin with background correction.

2.5 | Measurement of flippase activities in human RBCs

Flippase activity was determined by measuring PS internalization on purified RBCs using flow cytometry, in accordance with previously reported methods.[18] Basal flippase-independent flipping activity was determined after treating RBCs with 5 mM N-ethylmaleimide (NEM; Sigma-Aldrich) in PBS supplemented with glucose 0.2% (PBS-G) for 20 min at 37°C, which irreversibly and non-specifically inactivates flippases.[22] 1 µL of 1 mg/mL fluorescent PS (16:0–06:0 NBD-PS; Avanti Polar Lipids) was added to 1 mL of purified RBCs incubated in PBS-G at a hematocrit of 5% and incubated for 0–20 min at 37°C. Every 5 min, 20 µL of the upper suspension was washed with 1 mL PBS-G with 1% bovine serum albumin (BSA; Sigma-Aldrich) to remove remaining NBD-PS. Incubated RBCs were washed with 1 mL PBS-G. NBD-derived fluorescence was measured in duplicate by fluorescence activated cell sorting (BD FACSCanto II) of 100 000 cells per sample. The proportion of PS transported was calculated by dividing the fluorescence intensity of the inner leaflet by that of the loaded NBD-PS. Calculated fluorescent intensities were plotted, and the slope of the line was used as the NBD-PS transportation rate to calculate flippase activity.

2.6 | Measurements of PS surface exposure in human RBCs

PS surface exposure was determined by flow cytometry on purified RBCs. Because cellulose may decrease the amount of dense RBCs, whole blood collected in heparin tubes was centrifuged (1500 g, 10 min) to remove plasma, and the upper part of RBCs with buffy coat was collected and separated from the lower part of RBCs. This lower part was washed with NaCl 0.9% (1500 g, 5 min followed by 300 g, 10 min). The upper part of RBCs was separated from the buffy coat using a column filled with cellulose as described above. The lower and upper part were combined to form the total RBCs. Annexin V-fluorescein isothiocyanate (FITC) (BD Biosciences), diluted 20 times with Annexin V binding buffer (10 mM HEPES, 0.14 M NaCl, 2.5 mM $CaCl_2$) and incubated for 15 min at room temperature, was used for flow cytometry.

RBC storage stress experiments were performed to eliminate the influence of splenic removal of PS-exposing cells in vivo and to analyze PS surface exposure, in particular in the most dense RBCs. For this, part of the total RBCs were fractionized by density gradient centrifugation using 59%, 70%, and 78% Percoll (GE Healthcare). Total RBCs and fractions were tumbled for up to 2 days at 37°C in ringer buffer (32 mM HEPES pH 7.4, 1 mM MgSO4, 5 mM KCl, 125 mM NaCl) with and without glucose (5 mM) and/or Ca^{2+} ($CaCl_2$ 1 mM). In addition, apart from Annexin V-FITC also the Ca^{2+}-independent FITC-conjugated bovine lactadherin (BLAC-FITC; Haematologic Technologies, diluted in PBS) was used. Total RBCs and fractions (2% hematocrit) were diluted 20 times with (Annexin V binding or ringer) buffer and incubated 15 min at room temperature. Fluorescence levels of the total RBCs and fractions were quantified using flow cytometry and corrected for blanks without Annexin V-FITC or BLAC-FITC.

2.7 | RBC ion balance, membrane lipid composition, and distribution

Intracellular Ca^{2+} content was evaluated by microscopy, flow cytometry, and spectrofluorimetry after labeling of RBCs with the fluorescent marker Fluo-4 AM (Molecular Probes). For intracellular sodium (Na^+) and potassium (K^+) content, blood aliquots were collected into preweighed Eppendof tubes. They were washed three times in ice-cold Na^+/K^+-free solution containing 100 mM $Mg(NO_3)_2$ and 10 mM imidazole-HNO_3 (pH 7.4) and the buffy coat was aspirated. Weights of wet RBC pellets were recorded and samples were dried at 80°C for 3 days until constant weights were reached. Thereafter dry pellets were wet-burned in metal-free concentrated HNO_3. Na^+ and K^+ content were measured using a Sherwood flame photometer. Intracellular Na^+ and K^+ content was normalized to the dry weight of the RBC pellet.

The RBC membrane lipid composition, fatty acid, cholesterol, sphingolipid, and phospholipid contents including PS were determined by liquid chromatography–mass spectrometry (LC–MS) as previously reported.[23–25] Membrane lipid distribution at the RBC surface was analyzed in parallel by LC–MS and confocal live cell imaging to evaluate whether local changes in lipid domains could be revealed as previously described.[23,26] Membrane cholesterol content of washed RBCs was determined with a fluorescent assay kit (Invitrogen) and reported to the global Hb content.[26] To analyze the distribution of GM1 ganglioside and sphingomyelin, living RBCs were spread onto poly-L-lysine (PLL)-coated coverslips and then labeled by trace insertion in the plasma membrane of BODIPY-GM1 and -sphingomyelin fluorescent analogs

(Invitrogen).[27] Membrane cholesterol distribution was evidenced through living RBC labeling with mCherry-Theta toxin fragment followed by immobilization on PLL-coated coverslips.[26] Coverslips with living immobilized RBCs were placed in medium-filled LabTek chambers and observed with a wide-field fluorescence microscope (Zeiss Observer Z1; plan-Apochromat 100X 1.4 oil Ph3 objective).

2.8 | RBC morphology, deformability, density, markers of turnover, and flow properties

RBC morphology was determined on peripheral blood smears and by scanning electron microscopy of glutaraldehyde-fixed RBCs on filters. RBCs were prepared and analyzed as previously described.[23,26]

Osmotic fragility through Hb release and RBC deformability using osmotic gradient ektacytometry with the Laser Optical Rotational Red Cell Analyzer (Lorrca; RR Mechatronics) were used according to the manufacturer's instructions.[23,28]

Dense RBCs (Hb concentration > 41 g/dL) were measured on the ADVIA hematology analyzer (Siemens). RBC density separation was performed using the three Percoll gradients (59%, 70% and 78%) yielding four different fractions of RBCs according to density (i.e., cellular age) (from the top layer down to the bottom of the tube: fraction 1 containing the RBCs with the lowest density [i.e., youngest RBCs], up to fraction 4 containing the most dense RBCs [i.e., senescent RBCs]).[29]

Routine hematological parameters including reticulocyte counts were measured using a CELL-DYN Sapphire (Abbott Diagnostics). The RBC membrane protein ratio of band 4.1a to 4.1b was measured to determine the average RBC age. Band 4.1a:b ratio was quantified using densitometry as reported.[30,31] In short, after treatment of RBCs with di-isopropyl fluorophosphates, ghosts were prepared according to the method of Dodge.[32] Band 4.1a:b ratio was detected in RBC ghosts after protein separation by SDS-PAGE and visualization of protein bands using Coomassie blue staining.

To evaluate RBC flow properties and subtle changes in RBC morphology, a lab-on-a-chip-based point-of-care device, Erysense (Cysmic), was used.[33] This method uses machine learning algorithms to characterize single cell morphologies in microfluidic channels with rectangular cross-sections to simulate capillary flow. For deformable RBCs, geometric asymmetry of the cross-section of the channels results in two dominating morphologies depending on flow velocity (centered croissant-like cells at lower velocities and off-centered slipper-like cells at higher velocities). Distribution of the RBC lateral equilibrium position (y) along the channel width (W) for a given velocity is a characteristic indicator of single-cell flow.

3 | RESULTS

3.1 | Case presentation

A 37-year-old male with only a medical history of non-radicular low back pain presented with severe opioid-treated abdominal pain in the left upper quadrant, mild splenomegaly, and chronic fatigue since a short febrile episode 8 months before. He had reduced exercise capacity (early lactate threshold at 27% of predicted VO_2 evaluated by pulmonary function tests) without abnormalities on imaging studies of the chest including high resolution computed tomography, and a normal Hb-oxygen dissociation curve (p50 using a Hemox Analyzer). Abdominal ultrasound and computed tomography showed no gall stones or cholecystitis. Laboratory parameters showed: Hb 13.2 g/dL (normal 13.9–17.2), mean corpuscular volume 93 fL (80–97), reticulocytosis 194 $\times$ 10^9/L (25–120) (4.5%), increased total bilirubin 1.81 mg/dL (0.18–1.23), and erythropoietin 35 IU/L (3–32). During follow-up lactate dehydrogenase was once increased to 261 U/L (0–250) and haptoglobine ranged from 0.53 to 0.79 g/L (0.30–2.00). Altogether, we conclude that the patient suffered from mild hemolytic anemia. Acquired causes of hemolytic anemia were excluded, as were common hereditary causes such as Hb variants (HPLC), deficiencies of glucose-6-phopshate dehydrogenase and pyruvate kinase, and hereditary spherocytosis (osmotic gradient ektacytometry, EMA binding test). Subsequent analysis of 46 genes associated with hereditary hemolytic anemia revealed hemizygosity for a novel missense variant, c.2365C > T p.(Leu789Phe) in *ATP11C*. In addition, the patient was heterozygous for the α-spectrin (*SPTA1*) α^{LEPRA} variant. This is a relatively common cause of autosomal recessive hereditary spherocytosis (minor allele frequency 0.5%) and heterozygosity for this variant is not associated with a clinical phenotype.[15]

Leu789 is a highly conserved amino acid in the phosphorylation domain of ATP11C (Figure S1). The Leu789Phe variant was not reported earlier and absent in the Genome Aggregation Database (gnomAD).[34] In silico tools (SIFT, PolyPhen2 HumDiv and HumVar, PROVEAN, MutationTaster) predicted the variant to be deleterious. The variant was inherited from the patient's mother who was heterozygous and clinically unaffected.

3.2 | Decreased protein expression and ATPase activity of murine *Atp11c* mutant in HEK293T cells

To characterize the effects of the Leu789Phe variant in *ATP11C*, mutagenesis was performed. Protein sequence analysis showed that Leu789Phe in human ATP11C aligns with Leu786Phe in mouse Atp11c. These species have 98% homology in their ATP11C constructs. Expression levels in HEK293T cells of the equivalent murine mutant (Leu786Phe) were 27% ± 14% compared to WT (Figure 1A). ATPase activity of WT Atp11c was strongly activated by PS. In contrast, detergent-solubilized mutant protein showed reduced PS-stimulated ATPase activity, reflected by a 57% decrease in V_{max} of mutant Atp11c compared to WT (Figure 1B). Substrate affinity of the mutant protein was unaffected (Figure 1B). Together, these results imply that both the expression and the functional activity of the missense variant are significantly reduced relative to WT Atp11c.

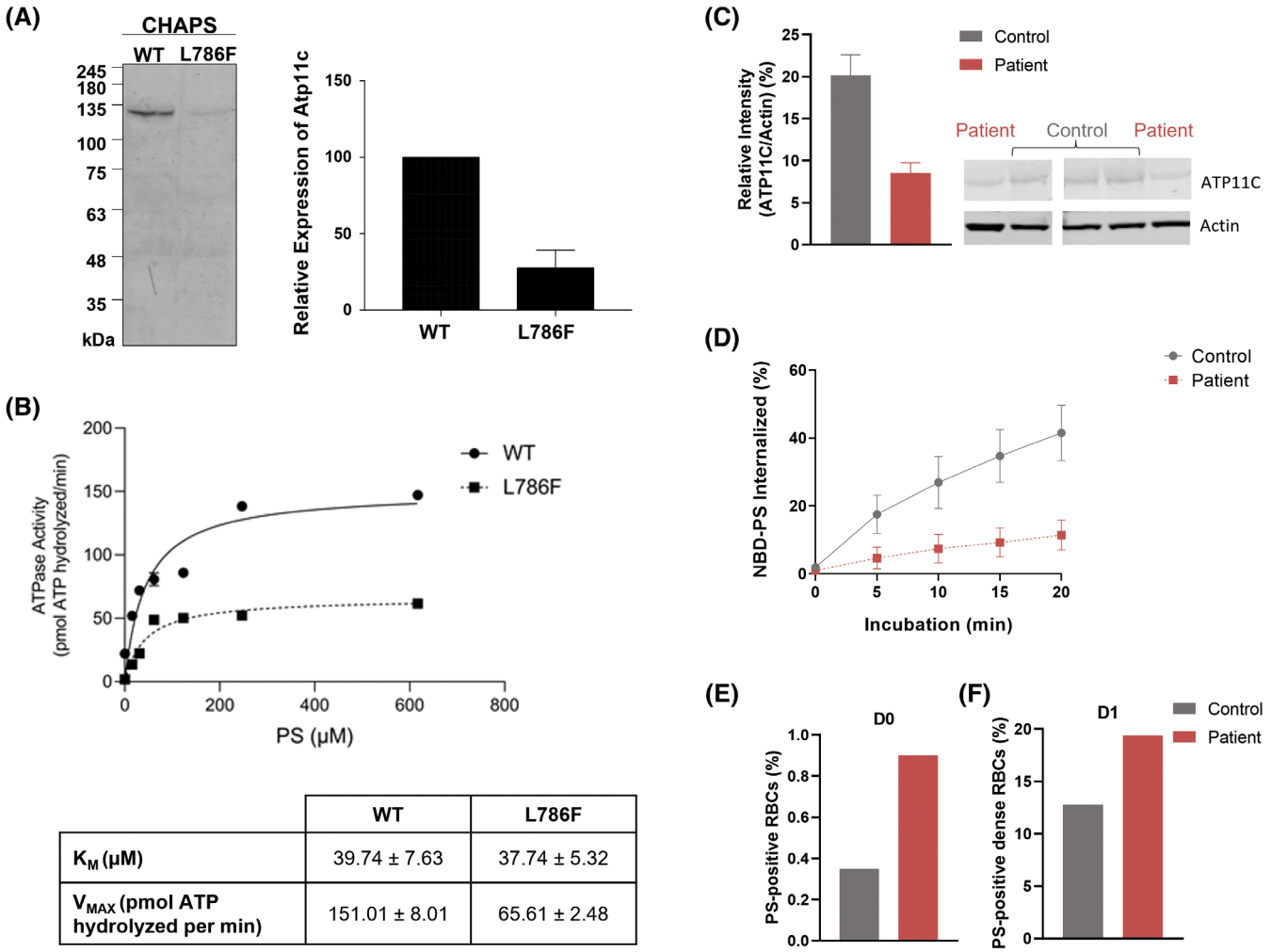

	WT	L786F
K_M (μM)	39.74 ± 7.63	37.74 ± 5.32
V_{MAX} (pmol ATP hydrolyzed per min)	151.01 ± 8.01	65.61 ± 2.48

FIGURE 1 Leu789Phe variant in *ATP11C* is associated with decreased red blood cell (RBC) flippase activity and increased phosphatidylserine (PS) exposure due to reduced ATP11C expression. (A) Immunoblot of recombinant mutant ATP11C murine protein harboring the equivalent Leu786Phe substitution showed expression levels that are approximately 27% compared to WT in HEK293T cells. Values are means ± standard deviation (SD) of $n = 5$ experiments. (B) PS titration ATPase assay on detergent-solubilized recombinant mutant protein (filled squares) showed decreased PS-stimulated activity compared to WT (filled circles). Data points were fitted with Michaelis-Menton curve to calculate K_m and V_{max}. Values are means ± SD of $n = 6$ measurements in $n = 2$ experiments. (C) Relative intensity of ATP11C calculated using actin as internal control in the patient and controls. Values are means ± SD of $n = 2$ experiments. (D) PS flipping activity measured in patient RBCs (filled squares) showed a 74% reduction in internalization of NBD-PS as compared to control RBCs (filled circles) after 20 min incubation. Values are means ± SD of $n = 2$ experiments with in total $n = 3$ controls. (E) Percentage of PS-positive RBCs (Annexin V-FITC) was increased in patient's total RBCs compared to control's total RBCs ($n = 1$) on the day of blood draw (D0). (F) In RBC storage stress experiments, 1 day after blood draw (D1) the percentage of PS-positive RBCs was further increased but differed only in the most dense RBCs (i.e., fraction 4 corresponding to the layer of Percoll 78%) of the patient compared to control ($n = 1$; Annexin V-FITC). However, this difference in PS exposure could only be detected in conditions when RBCs were tumbled at 37°C in ringer buffer in absence of glucose but presence of Ca^{2+}. ATP: adenosine triphosphate; ATPase, Adenosine Triphosphatase; ATP11C, Adenosine Triphosphatase Phospholipid Transporting 11C; CHAPS, 3-cholamidopropyl dimethylammonio 1-propanesulfonate; K_m, Michaelis–Menten constant; L786F, Leu786Phe; PS, phosphatidylserine; (NBD-)PS, (nitrobenzoxadiazole-labeled) phosphatidylserine; RBCs, red blood cells; V_{max}, maximum activity; WT, wild type. [Color figure can be viewed at wileyonlinelibrary.com]

3.3 | Patient RBCs have less ATP11C protein expression, reduced flippase activity, and mildly increased PS surface exposure

To evaluate the effect of the Leu789Phe variant on ATP11C expression in the patient, immunoblotting was performed. ATP11C expression in the patient was 42% decreased compared to controls (mean relative intensity was 8.6% ± 1.1% in the patient and 20.2% ± 2.4% in controls; Figure 1C). In line with this, patient RBCs displayed a 74% decrease in internalization of added PS relative to control RBCs (mean NBD-PS internalized 10.8% ± 3.5% in the patient and 41.1% ± 8.1% in controls; Figure 1D). In addition, PS surface exposure on the total population of patient RBCs was found to be 2.6-fold increased when compared to control RBCs (mean PS-positive RBCs 0.90%

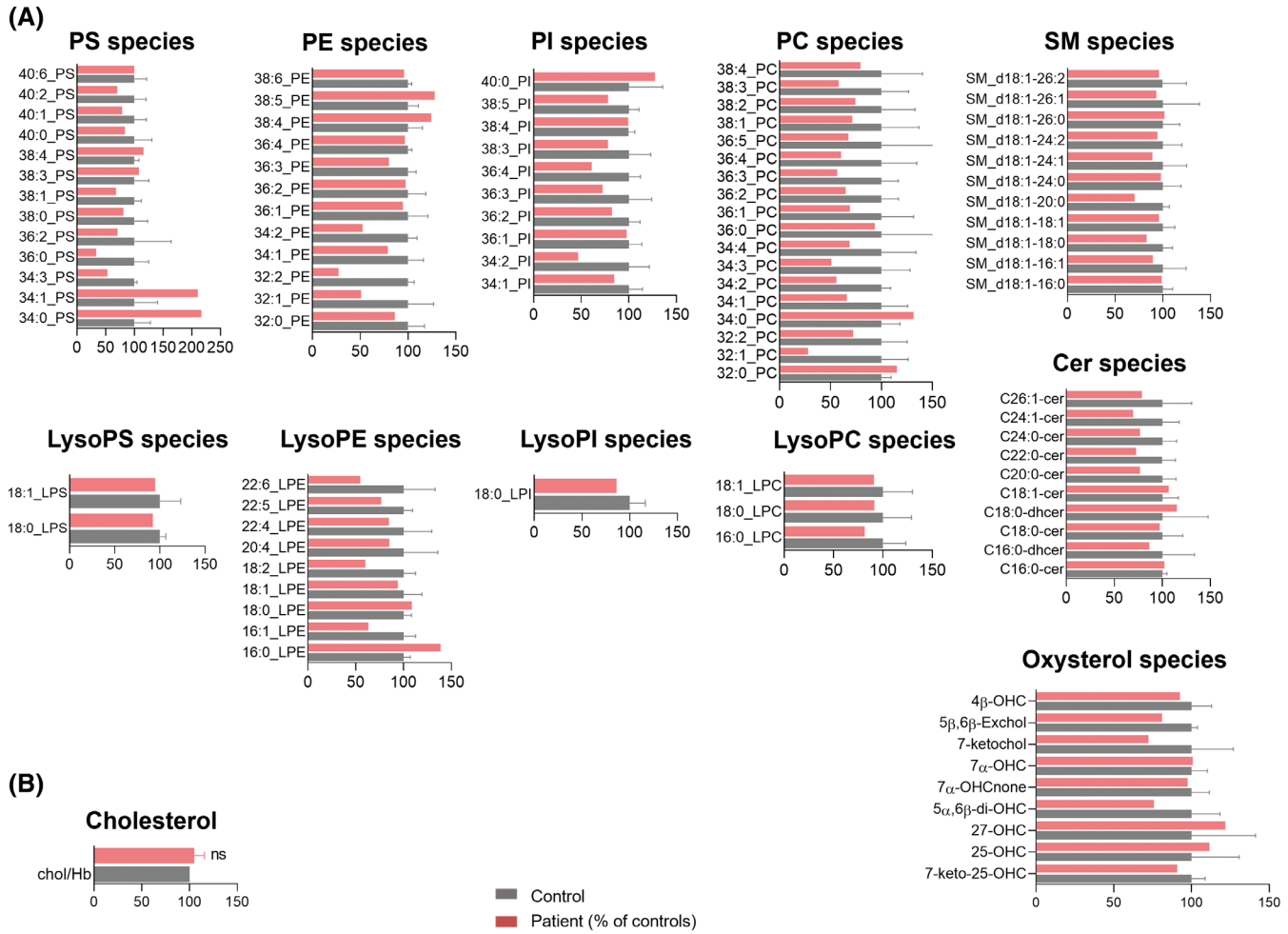

FIGURE 2 No obvious membrane lipid change is seen in the patient RBCs when normalized to controls, except a decrease of PC species and differential modulation of PS and PE species based on length and unsaturation. (A) Lipid species were assessed by HPLC-MS on washed, lysed, and lipid-extracted RBCs. Results are expressed as percentage of controls. Data in patient are means of three independent lysates from one experiment (red columns) and data in controls are means ± SD of three different donors each in triplicates (gray columns). (B) Cholesterol content determined through a fluorescent assay kit. Cholesterol content was normalized to Hb content and expressed as percentage of control RBCs. Mean ± SD of eight determinations. Cer, ceramide; ns, not significant; PC, phosphatidylcholine; PE, phosphatidylethanolamine; PI, phosphatidylinositol; PS, phosphatidylserine; RBC, red blood cell; SM, sphingomyelin. [Color figure can be viewed at wileyonlinelibrary.com]

vs. 0.35%; Annexin V-FITC; Figure 1E). RBC storage stress experiments showed that patient's PS exposure further increased on the first day after blood draw in the most dense RBCs (mean PS-positive dense RBCs 19.4% vs. 12.8%; Annexin V-FITC; Figure 1F). However, this difference was only found in absence of glucose but in presence of Ca^{2+} in the buffer (Figure S2; BLAC-FITC).

3.4 | Patient RBCs do not exhibit obvious changes in intracellular cation content nor in global RBC membrane PS content

Intracellular Ca^{2+} content was measured to evaluate whether the mild increase of PS surface exposure in patient RBCs could be associated with changes in scramblase activity. Independent of the method used, no definite changes in intracellular Ca^{2+} levels were seen (Figure S3). Intracellular cation content was also measured as it is known that a decrease in intracellular K^+ reduces flippase activity.[11] Intracellular Na^+ was slightly reduced, but intracellular K^+ content of patient RBCs did not obviously differ from that of controls (Figure S4).

In addition, the mild increase of PS surface exposure could also result from (1) reduced PS versus increased lysoPS levels, as previously shown in a patient with hereditary elliptocytosis;[35] and/or (2) increased levels of cholesterol, shown to contribute to the control of phospholipid asymmetry by inhibiting phospholipid scrambling.[9,26,36] We therefore compared the patient and control RBCs for phospholipids, lysophospholipids, sphingomyelins, ceramides, cholesterol, and oxysterol contents. However, there was no obvious difference in membrane lipid composition between patient and controls, except a general decrease of PC species and differential modulation of PS and PE species, based on length and unsaturation (Figure 2A,B).

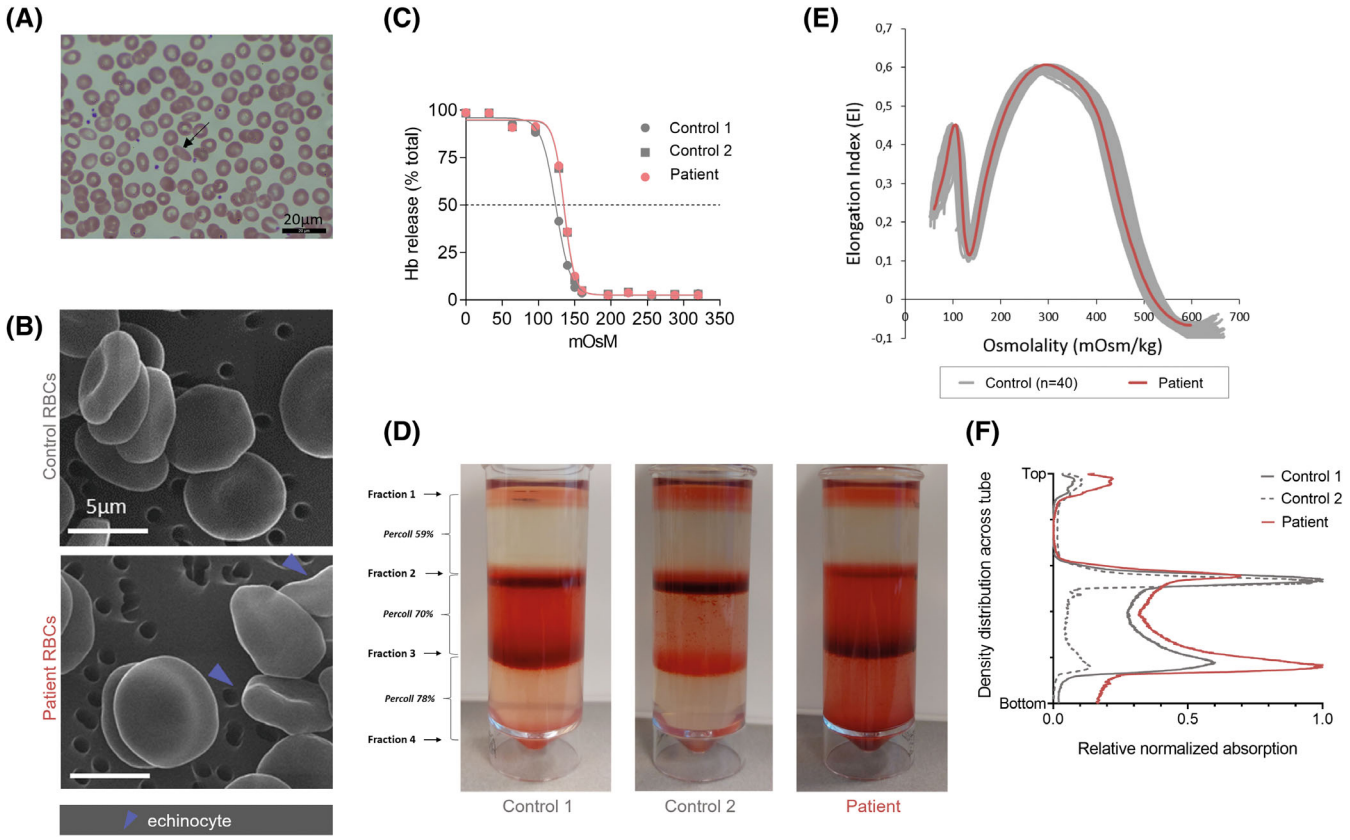

FIGURE 3 RBC morphology, fragility, deformability, and density-based fractionation. (A) Peripheral blood smear (May–Grünwald Giemsa stain) of the patient with the Leu789Phe variant in ATP11C showed mild polychromasia and occasional ovalocytes (black arrow) (Leica DM 3000 LED microscope, Leica Application Suite version 4.8). (B) Preservation of RBC morphology apart from some echinocytes visualized by scanning electron microscopy. (C) Preservation of resistance to hemolysis. (D) RBCs of the patient and controls ($n = 2$) were separated by Percoll-based density centrifugation with an equal volume of 2 mL PBS-diluted RBCs layered on three different Percoll gradients, yielding four different fractions (i.e., the formation of bands of cells at the interface of two different Percoll solutions). As visualized on these pictures, the patient showed more RBCs in the denser fraction 3 and 4 compared to controls. (E) Preservation of RBC deformability, expressed as the elongation index (EI) reflecting the total population of RBCs, under an osmotic gradient. (F) Profile of the cell distribution derived from intensity-based analysis and aligned with the pictures in panel F showed that patient had more RBCs in fraction 1 and 3 and less RBCs in fraction 2 compared to the controls. The density distribution refers to the cells on top of the tube to the lowest measurable position at the bottom of the tube. Fraction 4 could not be included in this analysis because of interference of the conical tube base. RBC, red blood cell. [Color figure can be viewed at wileyonlinelibrary.com]

To finally evaluate the possibility that such lipids could be differentially clustered at the RBC outer membrane, we determined the distribution and abundance of cholesterol-, GM1 ganglioside- and sphingomyelin-enriched domains.[27,37] Only cholesterol-enriched domains were significantly increased in patient RBCs by approximately twofold (Figure S5).

3.5 | Patient RBCs display more dense RBCs with a higher turnover and different morphology under flow without evidence for increased osmotic fragility or reduced deformability

Then, we wondered if the variant could have an impact on RBC morphology and deformability. RBC morphology of peripheral blood smears was unremarkable except for mild polychromasia and occasional ovalocytes (Figure 3A). Scanning electron microscopy showed preservation of RBC morphology apart from sporadic echinocytes (Figure 3B).

While RBC osmotic fragility and deformability were preserved (Figure 3C,E), a higher percentage of total dense cells was measured (3.3% of total RBCs in patient whole blood compared to 0.6 ± 0.4% in $n = 2$ controls). This was also reflected by more RBCs in fraction 3–4 after Percoll-based density centrifugation and a broader distribution of RBC fractions, which is generally a characteristic of RBCs of patients with hereditary hemolytic anemia (Figure 3D,F).[38]

Apart from a mild increase in reticulocyte count, a decreased 4.1a:b ratio was found in the patient compared to controls at two time points (0.78 vs. 1.14 ± 0.08 and 1.08 ± 0.03 vs. 1.66 ± 0.11). This indicates reticulocytosis due to increased RBC turnover.

In addition, a difference was seen in single cell flow characteristics of patient RBCs compared to control RBCs (Figure 4A). In

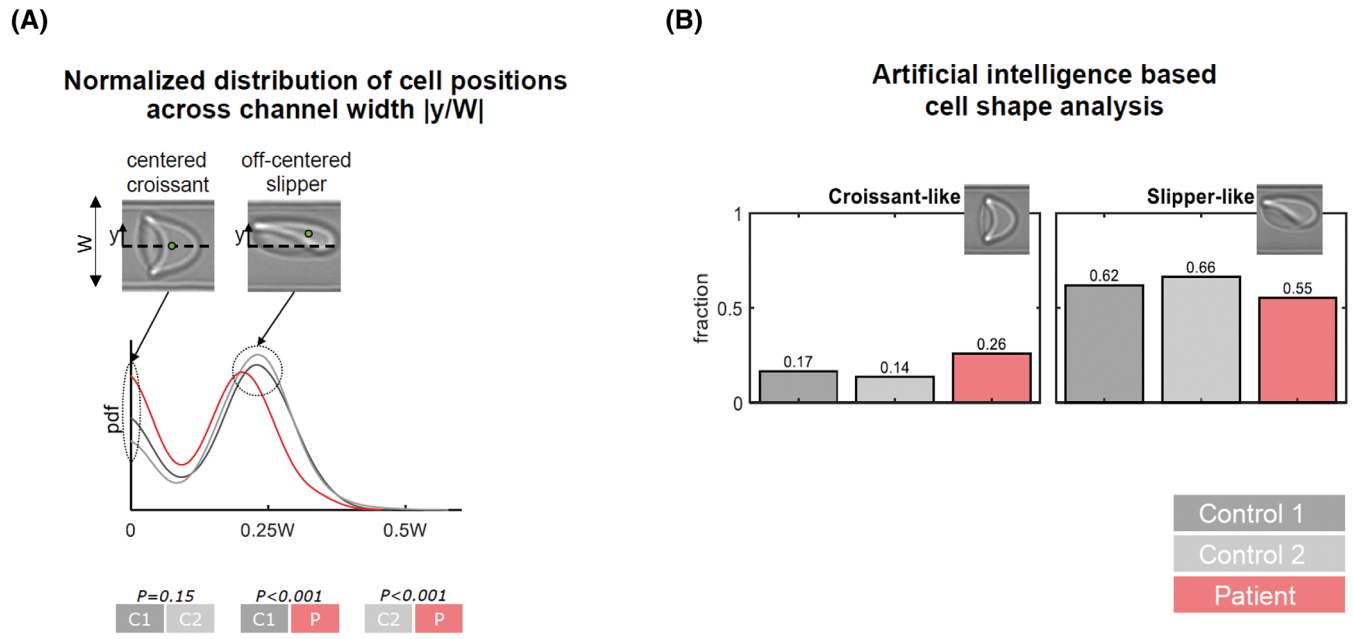

FIGURE 4 RBC morphology under flow. (A) Single cell analysis was performed in microfluidic, rectangular channels (y = lateral position, width [W] = 10 μm, height = 8 μm, pressure = 500 mbar, velocity of cell≈4 mm/s). Patient sample showed a higher fraction of RBCs that flowed in the center of the channel at $y = 0$ (probability density functions [pdf] of the normalized cell's center-of-mass in y-direction; p-values are derived from one-way ANOVA test with Tukey's multiple comparison). (B) Patient RBCs showed more croissant-like cell shapes when compared to control RBCs ($n = 2$, age and gender matched). RBC, red blood cell. [Color figure can be viewed at wileyonlinelibrary.com]

general, more centered croissant-like cell shapes were present in the patient (Figure 4B). Assuming that these differences reflect RBC properties in capillary flow, this could indicate an inability to transfer capillaries due to altered deformation, which in turn could lead to vaso-occlusion, pain crisis, and ischemia–reperfusion injury. This could be an attractive hypothesis in light of the severe chronic abdominal pain, but it remains to be further investigated and confirmed.

4 | DISCUSSION

A novel hemizygous missense variant, c.2365C > T p.(Leu789Phe), in *ATP11C* was found in a patient with mild hemolytic anemia. This variant led to a marked decrease in flippase activity in patient RBCs (74% reduction) and HEK293T cells expressing the equivalent murine mutant ATP11C protein (57% reduction). Decreased flippase activity was due to decreased ATP11C expression levels and decreased enzymatic function. Because ATP11C is the only abundant P4-ATPase in human RBCs, it is considered to play an important role in establishing and maintaining RBC membrane phospholipid asymmetry essential for RBC survival. Mild alterations in PS surface exposure, RBC morphology (under flow), density, and turnover were identified.

To date, only one patient with an *ATP11C* variant has been reported.[18] This other patient was hemizygous for the c.1253C > A p.(Thr418Asn) missense variant in *ATP11C*, and had a similarly mild hemolytic anemia, diagnosed at childhood, but no other complaints. Although our patient first presented at adult age after a febrile episode, his overall clinical picture seemed more severe with pronounced spleen pain, possibly related to phagocytosis of PS-positive RBCs by splenic macrophages, tiredness, and reduced physical capacity. Inflammation (i.e., febrile episode) at the onset of his complaints, triggering production of inflammatory mediators such as secretory phospholipase A_2 could have played a role by attacking PS-exposing RBCs.[39] This could have activated his reticuloendothelial system, which could elicited a vicious circle between hemolysis and inflammation. Such aggravation of hemolysis is well recognized in other hereditary hemolytic anemias.[40] Interestingly, older age is associated with increased PS surface exposure in ATP11C deficient mice, possibly leading to worsening of anemia.[17]

Arashiki et al. found in the other patient a larger, ten-fold instead of nearly fourfold decrease in flippase activity. In addition, an increase in PS surface exposure was only reported in the 0.1% most dense RBCs,[18] whereas we already found a mild increase in PS expression in the total RBC population. This may reflect differences in experimental settings, in potential alterations of transporter-lipid interactions by adding the polar, bulky NBD derivatives for flippase activity measurements, in the underlying variants on residual flipping activity of ATP11C, other known factors influencing flippase activity (e.g., intracellular ATP, K^+, or Ca^{2+} concentration) or compensatory activity of other flippases such as ATP11A and ATP11B.[8,11,41] Moreover, it is worth mentioning that in both patients, in presence of an active spleen, only PS exposing cells that escape removal by the spleen are measured. The fact that PS exposing cells are increased

after collection indicates that the normal recognition and removal of PS exposing cells is overwhelmed. Therefore, the measured percentage of PS exposing cells likely underestimates the formation of these cells in vivo. The more pronounced increase in PS seems to be in line with the more severe clinical phenotype in our case, although the hematological phenotype appears comparable.

We further investigated the marked decrease in flippase activity in RBCs by analysis of recombinant mutant ATP11C. We could strengthen our hypothesis that Leu789Phe variant is pathogenic based on decreased protein expression and enzymatic activity compared to wild type. Just like in humans, murine *Atp11c* variants have previously been associated with anemia.[17] Apart from anemia, mice with a loss-of-function variant in *ATP11C* showed stomatocytosis, but also alterations in cells other than RBCs, resulting in cholestasis, hepatocellular carcinoma and defects in B-cell maturation.[17,42] Contrary to mice deficient in ATP11C, no significant alterations of RBC shape, although we observed some under flow, or other cells were previously reported in humans.[17,18] However, this does not necessarily mean that variants in ATP11C only affect RBCs, especially in specific vulnerable conditions such as inflammation.

In addition, our research showed that RBCs of our patient seem to differ from normal, senescent RBCs and RBCs of other hereditary hemolytic anemias such as sickle cell disease, in which decreased flippase activity and/or increased PS exposure are associated with decreased intracellular K^+ and/or increased Ca^{2+} levels.[11,43,44] Probably, pathogenicity of the *ATP11C* variant reported here is solely due to premature aging of RBCs within the circulation by enhanced (i.e., accelerated) PS surface exposure. In RBC storage stress experiments without macrophage driven removal of PS-positive cells in the spleen, we could trigger PS surface exposure mainly in the most dense RBCs tumbled at 37°C in ringer buffer without glucose. Ca^{2+} was needed in the buffer, both when analyzing by Ca^{2+}-dependent binding of annexin V-FITC and Ca^{2+}-independent binding of BLAC-FITC, suggesting that PS is not exposed on RBC surfaces as long as scramblase is inactive, regardless of flippase activity. Thus, one should consider scramblase (in)activity as influencing factor of PS surface exposure.

Finally, we were able to identify subtle changes in domains of the outer membrane leaflet and RBC morphology, also under flow. The exact mechanisms and physiological relevance remain to be established, but could be related to altered biophysical, rheological, membrane stability, and oxygen delivery properties.[27,33,45]

In summary, we provide convincing evidence for the pathogenic nature of a novel c.2365C > T p.(Leu789Phe) missense variant in *ATP11C*. Our findings likely explain the hemolytic anemia in the patient but not his entire clinical phenotype. Although ATP11C deficiency is rare, it may be more frequent than the two cases currently known. This may be because of its mild clinical expression and the fact that *ATP11C* is not regularly part of many diagnostic Next Generation Sequencing gene panels.[46–48] Identification of more patients and genetic variants, combined with functional tests including flippase activity and PS surface exposure could aid in a better understanding of the phenotypic expression of ATP11C deficiency.

AUTHOR CONTRIBUTIONS

Myrthe J. van Dijk coordinated the project, collected data, performed experiments, performed analyses and wrote the manuscript; Brigitte A. van Oirschot, Alexander N. Harrison, Steffen M. Recktenwald, Min Qiao, Amaury Stommen, Anne-Sophie Cloos, Juliette Vanderroost, Romano Terrasi, Kuntal Dey, Jennifer Bos, Minke A.E. Rab, Anna Bogdanova, Giampaolo Minetti, Giulio G. Muccioli, Donatienne Tyteca, Stéphane Egée, Lars Kaestner, and Robert S. Molday performed experiments and analyses and reviewed the manuscript; Eduard J. van Beers collected data and reviewed the manuscript; Richard van Wijk coordinated the project, supervised the project and reviewed the manuscript. All authors approved the final version of the manuscript.

ACKNOWLEDGMENTS

The authors would like to thank the patient and his family member for the collaboration. We also like to thank Prof. Nakamura and Dr. Arashiki (Tokyo Women's Medical University, Tokyo, Japan) for providing conditioned medium from the 11C4 clone of the anti-ATP11C monoclonal antibody.

CONFLICT OF INTEREST STATEMENT

Steffen M. Recktenwald and Lars Kaestner are shareholders of Cysmic GmbH, the manufacturer of Erysense, which was used to generate the data in Figure 4. The remaining authors have no relevant conflicts of interest to disclose and declare that the research was conducted in the absence of any competing financial interests.

DATA AVAILABILITY STATEMENT

The data that support the findings of this study are available on request from the corresponding author. The data are not publicly available due to privacy or ethical restrictions.

ORCID

Myrthe J. van Dijk https://orcid.org/0000-0002-9377-0367
Alexander N. Harrison https://orcid.org/0000-0002-7290-4725
Steffen M. Recktenwald https://orcid.org/0000-0003-1235-1521
Min Qiao https://orcid.org/0000-0002-2734-6824
Amaury Stommen https://orcid.org/0000-0003-4761-8521
Kuntal Dey https://orcid.org/0000-0001-6590-2804
Anna Bogdanova https://orcid.org/0000-0003-0502-5381
Giampaolo Minetti https://orcid.org/0000-0003-3063-4613
Donatienne Tyteca https://orcid.org/0000-0002-7334-2648
Lars Kaestner https://orcid.org/0000-0001-6796-9535
Robert S. Molday https://orcid.org/0000-0002-4479-1831
Eduard J. van Beers https://orcid.org/0000-0002-3934-7189
Richard van Wijk https://orcid.org/0000-0002-8236-8292

REFERENCES

1. Alaarg A, Schiffelers RM, van Solinge WW, van Wijk R. Red blood cell vesiculation in hereditary hemolytic anemia. *Front Physiol*. 2013;4-(Article 365):1-15.
2. Zwaal RFA, Comfurius P, Bevers EM. Surface exposure of phosphatidylserine in pathological cells. *Cell Mol Life Sci*. 2005;62(9):971-988.

3. Mohandas N, Gallagher PG. Red cell membrane: past, present, and future. *Blood*. 2008;112(10):3939-3948.
4. Boas FE, Forman L, Beutler E. Phosphatidylserine exposure and red cell viability in red cell aging and in hemolytic anemia. *Proc Natl Acad Sci U S A*. 1998;95(6):3077-3081.
5. Connor J, Pak CC, Schroit AJ. Exposure of phosphatidylserine in the outer leaflet of human red blood cells. Relationship to cell density, cell age, and clearance by mononuclear cells. *J Biol Chem*. 1994;269(4):2399-2404.
6. Andersen JP, Vestergaard AL, Mikkelsen SA, Mogensen LS, Chalat M, Molday RS. P4-ATPases as phospholipid flippases—structure, function, and enigmas. *Front Physiol*. 2016;7:7.
7. Clark K, Karsch-Mizrachi I, Lipman DJ, Ostell J, Sayers EW. GenBank. *Nucleic Acids Res*. 2016;44(D1):D67-D72.
8. Liou AY, Molday LL, Wang J, Andersen JP, Molday RS. Identification and functional analyses of disease-associated P4-ATPase phospholipid flippase variants in red blood cells. *J Biol Chem*. 2019;294(17):6809-6821.
9. Arashiki N, Takakuwa Y. Maintenance and regulation of asymmetric phospholipid distribution in human erythrocyte membranes: implications for erythrocyte functions. *Curr Opin Hematol*. 2017;24(3):167-172.
10. Segawa K, Kurata S, Nagata S. The CDC50A extracellular domain is required for forming a functional complex with and chaperoning phospholipid flippases to the plasma membrane. *J Biol Chem*. 2018;293(6):2172-2182.
11. Seki M, Arashiki N, Takakuwa Y, Nitta K, Nakamura F. Reduction in flippase activity contributes to surface presentation of phosphatidylserine in human senescent erythrocytes. *J Cell Mol Med*. 2020;24:13991-14000.
12. Wood BL, Gibson DF, Tait JF. Increased erythrocyte phosphatidylserine exposure in sickle cell disease: flow-cytometric measurement and clinical associations. *Blood*. 1996;88(5):1873-1880.
13. Kuypers FA, Yuan J, Lewis RA, et al. Membrane phospholipid asymmetry in human thalassemia. *Blood*. 1998;91(8):3044-3051.
14. Daleke DL. Regulation of phospholipid asymmetry in the erythrocyte membrane. *Curr Opin Hematol*. 2008;15(3):191-195.
15. Chonat S, Risinger M, Sakthivel H, et al. The spectrum of SPTA1-associated hereditary spherocytosis. *Front Physiol*. 2019;10:815.
16. Bogusławska DM, Machnicka B, Hryniewicz-Jankowska A, Czogalla A. Spectrin and phospholipids—the current picture of their fascinating interplay. *Cell Mol Biol Lett*. 2014;19(1):158-179.
17. Yabas M, Coupland LA, Cromer D, et al. Mice deficient in the putative phospholipid flippase Atp11c exhibit altered erythrocyte shape, anemia, and reduced erythrocyte life span. *J Biol Chem*. 2014;289(28):19531-19537.
18. Arashiki N, Takakuwa Y, Mohandas N, et al. ATP11C is a major flippase in human erythrocytes and its defect causes congenital hemolytic anemia. *Haematologica*. 2016;101(5):559-565.
19. Weiss MM, Van der Zwaag B, Jongbloed JDH, et al. Best practice guidelines for the use of next-generation sequencing applications in genome diagnostics: a national collaborative study of dutch genome diagnostic laboratories. *Hum Mutat*. 2013;34(10):1313-1321.
20. Wang J, Molday LL, Hii T, et al. Proteomic analysis and functional characterization of P4-ATPase phospholipid flippases from murine tissues. *Sci Rep*. 2018;8(1):2-15.
21. Vorselen D, van Dommelen SM, Sorkin R, et al. The fluid membrane determines mechanics of erythrocyte extracellular vesicles and is softened in hereditary spherocytosis. *Nat Commun*. 2018;9(1):4960.
22. Kuypers FA, Lewis RA, Hua M, et al. Detection of altered membrane phospholipid asymmetry in subpopulations of human red blood cells using fluorescently labeled annexin V. *Blood*. 1996;87(3):1179-1187.
23. Cloos A-S, Daenen LGM, Maja M, et al. Impaired cytoskeletal and membrane biophysical properties of acanthocytes in hypobetalipoproteinemia—a case study. *Front Physiol*. 2021;12:1-22.
24. Bottemanne P, Paquot A, Ameraoui H, Alhouayek M, Muccioli GG. The α/β–hydrolase domain 6 inhibitor WWL70 decreases endotoxin-induced lung inflammation in mice, potential contribution of 2-arachidonoylglycerol, and lysoglycerophospholipids. *FASEB J*. 2019;33(6):7635-7646.
25. Bottemanne P, Paquot A, Ameraoui H, Guillemot-Legris O, Alhouayek M, Muccioli GG. 25-hydroxycholesterol metabolism is altered by lung inflammation, and its local administration modulates lung inflammation in mice. *FASEB J*. 2021;35(4):e21514.
26. Cloos A-S, Ghodsi M, Stommen A, et al. Interplay between plasma membrane lipid alteration, oxidative stress and calcium-based mechanism for extracellular vesicle biogenesis from erythrocytes during blood storage. *Front Physiol*. 2020;11:11.
27. Conrard L, Stommen A, Cloos A-S, et al. Spatial relationship and functional relevance of three lipid domain populations at the erythrocyte surface. *Cell Physiol Biochem*. 2018;51(4):1544-1565.
28. Da Costa L, Suner L, Galimand J, et al. Diagnostic tool for red blood cell membrane disorders: assessment of a new generation ektacytometer. *Blood Cells Mol Dis*. 2016;56(1):9-22.
29. Rennie CM, Thompson S, Parker AC, Maddy A. Human erythrocyte fractionation in "percoll" density gradients. *Clin Chim Acta*. 1979;98(1–2):119-125.
30. Bogdanova A, Mihov D, Lutz H, Saam B, Gassmann M, Vogel J. Enhanced erythro-phagocytosis in polycythemic mice overexpressing erythropoietin. *Blood*. 2007;110(2):762-769.
31. Maurer F, John T, Makhro A, et al. Continuous Percoll gradient centrifugation of erythrocytes—explanation of cellular bands and compromised age separation. *Cell*. 2022;11(8):1296.
32. Dodge JT, Mitchell C, Hanahan DJ. The preparation and chemical characteristics of hemoglobin-free ghosts of human erythrocytes. *Arch Biochem Biophys*. 1963;100(1):119-130.
33. Recktenwald SM, Lopes MGM, Peter S, et al. Erysense, a lab-on-a-chip-based point-of-care device to evaluate red blood cell flow properties with multiple clinical applications. *Front Physiol*. 2022;13:1-10.
34. Karczewski KJ, Francioli LC, Tiao G, et al. The mutational constraint spectrum quantified from variation in 141,456 humans. *Nature*. 2020;581(7809):434-443.
35. Pollet H, Cloos A-S, Stommen A, et al. Aberrant membrane composition and biophysical properties impair erythrocyte morphology and functionality in elliptocytosis. *Biomolecules*. 2020;10(8):1120.
36. van Zwieten R, Bochem AE, Hilarius PM, et al. The cholesterol content of the erythrocyte membrane is an important determinant of phosphatidylserine exposure. *Biochim Biophys Acta*. 2012;1821(12):1493-1500.
37. Leonard C, Conrard L, Guthmann M, et al. Contribution of plasma membrane lipid domains to red blood cell (re)shaping. *Sci Rep*. 2017;7(1):4264.
38. Bogdanova A, Kaestner L, Simionato G, Wickrema A, Makhro A. Heterogeneity of red blood cells: causes and consequences. *Front Physiol*. 2020;11:392.
39. Neidlinger NA, Larkin SK, Bhagat A, Victorino GP, Kuypers FA. Hydrolysis of phosphatidylserine-exposing red blood cells by secretory phospholipase A2 generates lysophosphatidic acid and results in vascular dysfunction. *J Biol Chem*. 2006;281(2):775-781.
40. Zaninoni A, Fermo E, Vercellati C, Marcello AP, Barcellini W, Bianchi P. Congenital hemolytic anemias: is there a role for the immune system? *Front Immunol*. 2020;11:11.
41. Devaux PF, Fellmann P, Hervé P. Investigation on lipid asymmetry using lipid probes: comparison between spin-labeled lipids and fluorescent lipids. *Chem Phys Lipids*. 2002;116(1–2):115-134.

42. Yabas M, Teh CE, Frankenreiter S, et al. ATP11C is critical for the internalization of phosphatidylserine and differentiation of B lymphocytes. *Nat Immunol*. 2011;12(5):441-449.
43. Hertz L, Huisjes R, Llaudet-Planas E, et al. Is increased intracellular calcium in red blood cells a common component in the molecular mechanism causing anemia? *Front Physiol*. 2017;8:673.
44. Weiss E, Rees DC, Gibson JS. Role of calcium in phosphatidylserine externalisation in red blood cells from sickle cell patients. *Anemia*. 2011;2011:1-8.
45. Manno S, Takakuwa Y, Mohandas N. Identification of a functional role for lipid asymmetry in biological membranes: phosphatidylserine-skeletal protein interactions modulate membrane stability. *Proc Natl Acad Sci U S A*. 2002;99(4):1943-1948.
46. Russo R, Andolfo I, Manna F, et al. Multi-gene panel testing improves diagnosis and management of patients with hereditary anemias. *Am J Hematol*. 2018;93(5):672-682.
47. Roy NBA, Wilson EA, Henderson S, et al. A novel 33-gene targeted resequencing panel provides accurate, clinical-grade diagnosis and improves patient management for rare inherited anaemias. *Br J Haematol*. 2016;175(2):318-330.
48. Fermo E, Vercellati C, Marcello AP, et al. Targeted next generation sequencing and diagnosis of congenital hemolytic anemias: a three years experience monocentric study. *Front Physiol*. 2021;12:684569.

SUPPORTING INFORMATION

Additional supporting information can be found online in the Supporting Information section at the end of this article.

How to cite this article: van Dijk MJ, van Oirschot BA, Harrison AN, et al. A novel missense variant in *ATP11C* is associated with reduced red blood cell phosphatidylserine flippase activity and mild hereditary hemolytic anemia. *Am J Hematol*. 2023;98(12):1877-1887. doi:10.1002/ajh.27088